www.czasopisma.pan.pl PAN POLSKA AKADEMIA NAUK www.journals.pan.pl

Arch. Metall. Mater. **69** (2024), 1, 303-308

DOI: https://doi.org/10.24425/amm.2024.147823

M. NADOLSKI[1*], Ł. BERNAT[2], D. CEKUS[3], P. KWIATOŃ[3], A. PIETRZAK[4]

ANALYSIS OF COOLING A PRINTED 3D MOLD USING A CASTING AND SOLIDIFICATION SIMULATION OF A CUSN20 BRONZE BELL CASTING

The work done in this study is a preliminary investigation into the possibility of modelling the filling and solidification process of castings in molds made with the additive method. The work originated from an experiment to produce a bronze casting with a high tin content in an additive mold. The mold filling and solidification simulation was carried out in the MAGMASOFT program, and the lambda thermal conductivity coefficient used in the program's material database was corrected based on the actual temperature values of the printed form. The results were compared with the modeling results for the physical properties of furan molds based on the program database. The microstructure of the castings obtained in the compared forms was assessed.

Keywords: Fran mold; sand-base 3D printing; bell bronze; 3D printing; casting; solidification

1. Introduction

The development of additive manufacturing (AM) techniques observed in recent years offers new opportunities for the foundry industry. Models are made this way for molding technologies, in the investment technology but also directly from the molding compound. Historically, research into AM technology began in the early 1980s [1] with the development of the stereolithography (SL) [2] process, which 3D Systems Inc. later commercialized [3]. In essence, one could posit that AM technologies are finding applications in all industries using their speed, repeatability and print accuracy features [4], and additive manufacturing itself has been listed as one of the "key industrial sectors" [5]. The foundry industry also uses AM techniques to complement traditional alternatives, such as casting patterns for hand casting or the cast pattern method in precision foundries or micro-models for jewellery [6,7]. The advantage of AM, as opposed to traditional manufacturing methods, is that the manufactured elements may have complex shapes in the finished state [8,9]. In addition, a characteristic feature of additive manufacturing is a high degree of individualization and complexity of products, which translates into mass production of individual parts without a large increase in costs [10]. Due to the wide access to 3D printers, it is possible to print a form made in a CAD program in just a few hours, without the need to use mold patterns [11]. The possibility of making casting cores or molds using AM technology is also known [12]. The binders used in these techniques include alkyd, furan or silicate resins [13,14]. As new technologies and their potential applications develop, the materials' unique properties must be considered [15]. Studies on the influence of the cross-section of bells on their acoustic properties revealed the problem of so-called "human error", i.e., unintentional interference by the mold maker in the geometry of the mold [16,17]. The use of AM techniques has provided the opportunity to eliminate human error in making traditional bell-casting molds while forcing a change in mold technology. Initially, the rotating model was replaced by a bell-casting model. This direction of the proposed changes initially gave promising results, which, after acoustic analyses, turned out to be lower than expected. It was therefore decided to investigate the possibility of directly making casting molds using the additive method of sand with furan resin.

[1] CZESTOCHOWA UNIVERSITY OF TECHNOLOGY, FACULTY OF PRODUCTION ENGINEERING AND MATERIALS, DEPARTMENT OF METALLURGY AND METAL TECHNOLOGY, 42-200 CZESTOCHOWA, POLAND
[2] POZNAN UNIVERSITY OF TECHNOLOGY, FACULTY OF MECHANICAL ENGINEERING, INSTITUTE OF MATERIALS TECHNOLOGY, DIVISION OF FOUNDRY AND PLASTIC WORKING, 60-965 POZNAN, POLAND
[3] CZESTOCHOWA UNIVERSITY OF TECHNOLOGY, FACULTY OF MECHANICAL ENGINEERING AND COMPUTER SCIENCE, DEPARTMENT OF MECHANICS AND MACHINE DESIGN FUNDAMENTALS, 42-200 CZESTOCHOWA, POLAND
[4] AGH UNIVERSITY OF KRAKÓW, FACULTY OF FOUNDRY ENGINEERING, DEPARTMENT OF FOUNDRY, AL. MICKIEWICZA 30, 30-059 KRAKOW, POLAND
* Corresponding author: maciej.nadolski@pcz.pl

2. Research methodology

The bell was cast from CuSn20 bronze with a weight of 6 kg in a form made of quartz sand with furan resin, the pouring temperature was 1040°C. Copper and tin of high purity constituted feedstock. The die casting mold from the compound on the base of quartz sand with furan resin was made by means of the additive 3D printing technique. No fire-resistant coating was applied to the mold surface prior to the pouring process. The shape of an external mold with a constant thickness of 20 mm on the cross-section and an internal mold with a duct for the outflow of gases is shown in Fig. 1a. The temperature of the mold surface was controlled with a thermocouple type K in the vicinity of the largest mold cavity diameter – Fig. 1b. The initial temperature of the mold was 20°C, and during casting solidification the value was: after 1'30" – approx. 30°C, after 2'00" approx. 45°C, and after 4'30" approx. 140°C, respectively. The obtained casting was put under visual assessment – Fig. 1c. The observed changes in mold temperature during casting solidification in the new mold material resulting from 3D printing prompted the authors to undertake the examination of the mold priming and casting solidification process based on the adjusted thermal conductivity coefficient in the MAGMASOFT simulation software to values consistent with the observation. The results of the validation with the adjusted thermal conductivity coefficient were compared with the results of the modelling for the software available in the database with furan compound.

The following parameters of simulation tests were adopted for molds made of furan compound and for molds made of furan compound made in 3D technology (TABLE 1).

Tests to validate the mold cavity filling and solidification process were performed by means of the MAGMASOFT v5.5 simulation software. The values of thermophysical properties of the mold material from the MAGMASOFT software database were adopted and the obtained results were compared with the experimental values of the mold surface temperature – Fig. 2. It was observed that the default values of thermal conductivity for furan compound used in the material database are too high for the molds that were produced in the additive technique, hence the calculated temperature values are significantly higher than the actual measurements.

TABLE 1

Initial parameters of the simulation

Parameter	Value
Foundry alloy	CuSn20
Mold material	Furan: (silica sand + furan)
Liquidus temperature*	889°C
Solidus temperature*	818°C
Pouring temperature	1040°C
Mold temperature	20°C
Pouring time**	20 s
Filling tank level	90%
Number of cells	2 995 680
Number of cells in the cast	143 532

* – data based on own research (thermal derivative analysis) [12]
** – pouring time according to the experiment

Whereas the temperature value of the casting mold measured during the experiment was not consistent with the value obtained from the simulation, the value of the mold thermal conductivity coefficient was adjusted to obtain the mold surface temperature values consistent with the experiment. Reducing this value by 50% allowed numerical modelling to be carried out as closely as possible to the course of the experiment. The graph of the change in the value of the thermal conductivity parameter of furan compound before and after validation is presented in Fig. 3.

After the simulation, one which took into account the change of the molding weight lambda parameter, the temperature values on the outer part of the mold were obtained, which are presented in Fig. 4.

The conducted validation makes it possible to select molding compound parameters in such a way that they are as close as possible to the actual conditions. Figs. 5a and 5b show the distribution of the casting temperature during filling the mold cavity depending on the thermal conductivity parameters. On the left, values according to MAGMASOFT; on the right, after validation.

While analyzing the mold cavity filling process shown in Figs. 5a and 5b, it can be stated that this process was proceeding in a turbulent manner with the separation of the stream of liquid alloy. Such a method of filling may cause leaching of the molding compound and further occurrence of non-metallic inclusions

Fig. 1. The course of the experiment a) mold cross-section, b) mold during pouring, c) finished casting

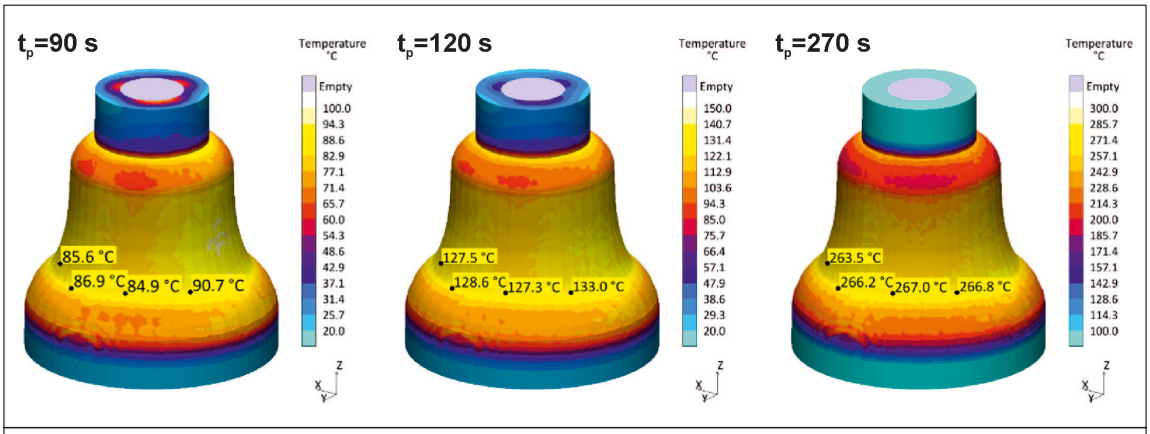

Maximum temperature of the mold surface from the simulation/experiment [°C]		
90.7 / 30	133.0 / 45	267.0 / 140

Fig. 2. Mold surface temperature (t_p – time from the moment of pouring the mold)

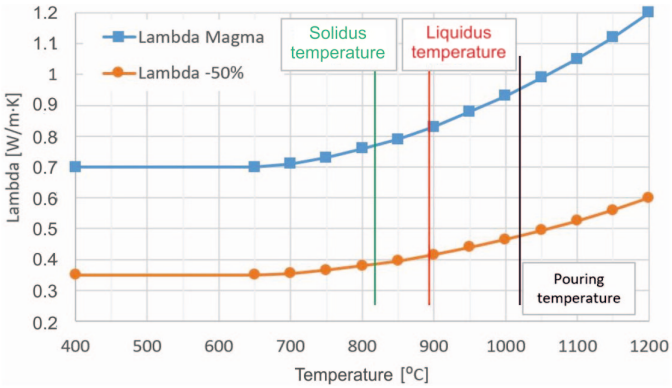

Fig. 3. Changes in the value of the thermal conductivity parameter of furan mass before and after validation

and discontinuities in the casting, such as oxide inclusions and porosity. The geometry of the mold with the molding compound parameters applied with a furan binder affects the temperature distribution of the stream, which is particularly visible for fillings from 20 to 50%. While analyzing the differences in the temperature in the casting after its solidification for two variants of mold formation and the corresponding lambda parameters, the difference is approx. 40-50°C. This difference affects the location of the porosity in the casting, as shown in Fig. 6.

The locations of the predicted shrinkage defects are located in places that do not necessarily solidify last. In the explanation of the mechanism of internal defects, it is useful to analyze the thermal module (Feedmod) – a scratch and the 'Hot Spot' criterion, which identifies areas with solidification times significantly different from the environment.

Feedmod – Fig. 7 can help to understand the thermal conditions within the casting. In comparison to the geometrical modulus (V/A), the thermal modulus takes "sand edge" effects and chills into account, which leads to a decrease or increase in the effective casting surfaces available for cooling and thus to different solidification times. Therefore, a more precise evaluation is possible with the thermal modulus than with the geometrical modulus. The 'Hot Spot' – Fig. 8 criterion shows those areas whose solidification times differ significantly from their surroundings. It thus helps you to identify where residual melt is surrounded by cooler material. As these areas are possibly cut off from feeding, there is a risk of shrink hole and porosity formation. What is more, you can also check directional solidification and thus identify potentially problem zones.

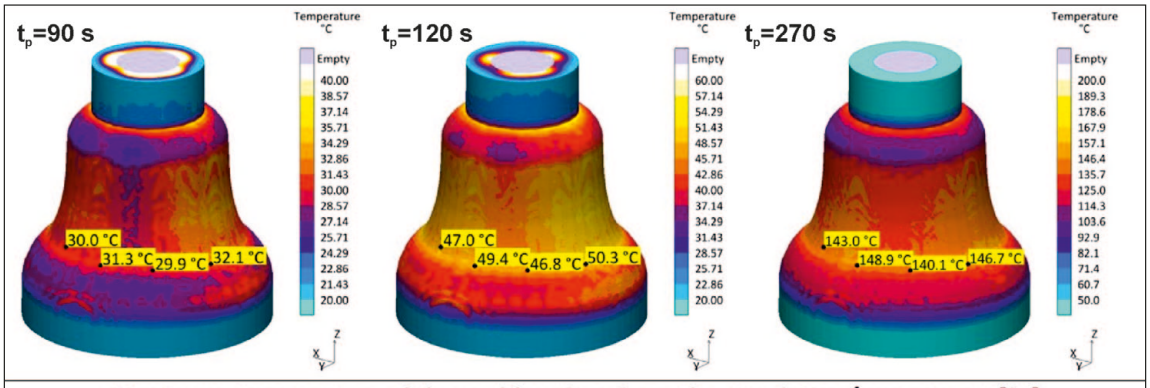

Maximum temperature of the mold surface from the simulation/experiment [°C]		
32.1 / 30	50.3 / 45	148.9 / 140

Fig. 4. Mold surface temperature (with variable molding weight lambda parameter; t_p – time from the moment of pouring the mold)

Fig. 5a. The distribution of the casting temperature when filling the mold cavity (pouring 10% to 60%)

The thermal module considers the effects of heat exchange between the casting and the grain of sand. Additionally, a feed effect is applied from the later solidifying areas. The feeding of solidifying casting proceeds in two directions: according to gravity, supplementing the metal shortage in the thickest part of the casting and in the horizontal direction, where the cross-section is the smallest – during solidification, there is a shortage of liquid metal due to shrinkage, that is to say, porosity, between the upper part of the casting fed from the main filler and the lower thickest part of the cross-section.

Observation and assessment of the microstructure of samples taken from castings made in furan compound and 3D printed mold was carried out. Samples were taken from the thickest parts of the casting. The metallographic samples were etched in $FeCl_3$ solution – Fig. 9. The structure of the obtained alloy consists of a soft plastic phase α and a mixture of eutectoid phase α and a hard intermetallic compound δ ($Cu_{31}Sn_8$). A finer structure was disclosed for the molding stock sample with furan binder than for the printed mold samples. This is due to the difference in the rate at which the heat is received from the solidifying alloy. Slower heat reception promotes the growth of dendrites. Precipitation measurements were made on 20 microstructures, analyzing 5 precipitates each.

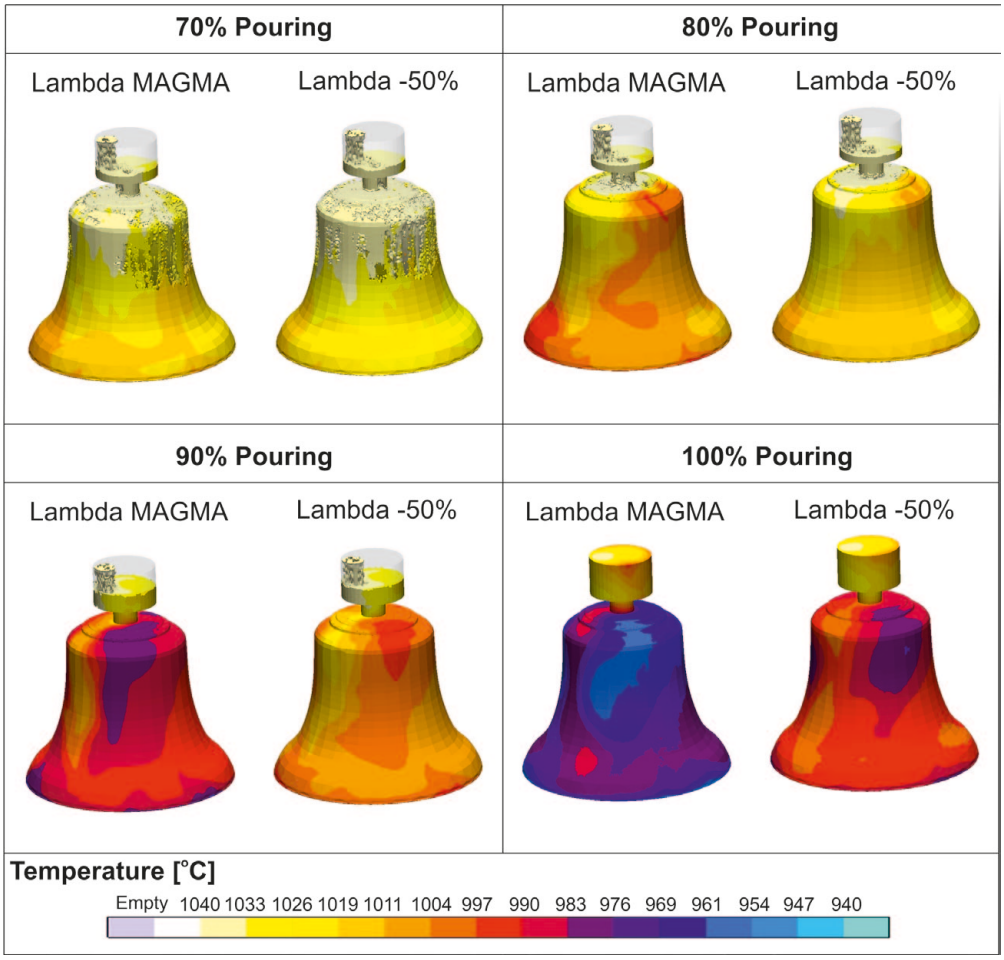

Fig. 5b. The distribution of the casting temperature when filling the mold cavity (pouring 70% to 100%)

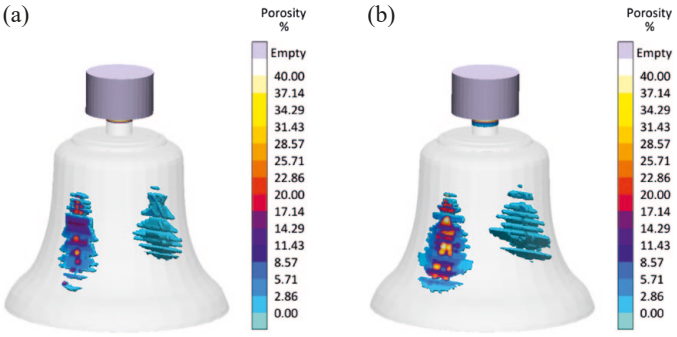

Fig. 6. Porosity in the casting: a) Lambda MAGMASOFT, b) Lambda validation

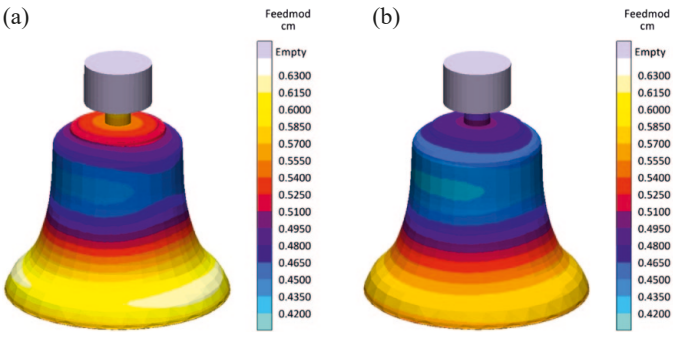

Fig. 7. Feedmod comparison: a) Lambda MAGMASOFT, b) Lambda validation

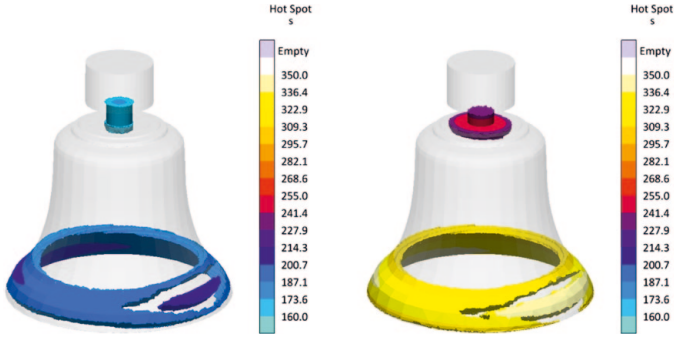

Fig. 8. Hot spot comparison

3. Conclusions

On the basis of experimental tests, the thermal conductivity coefficient of the sand mold with furan binder formed in the 3D printing process was determined and verified. It has been shown that with the same parameters of pouring the mold, the solidification time in printed molds is longer, which affects the bronze microstructure. Feedmod and Hot Spot analyses allow one to understand the mechanism of internal defects in the casting, allowing him or her to effectively counteract them.

The structure of the cast made in printed form shows larger phase separations α as compared to the mold made of furan

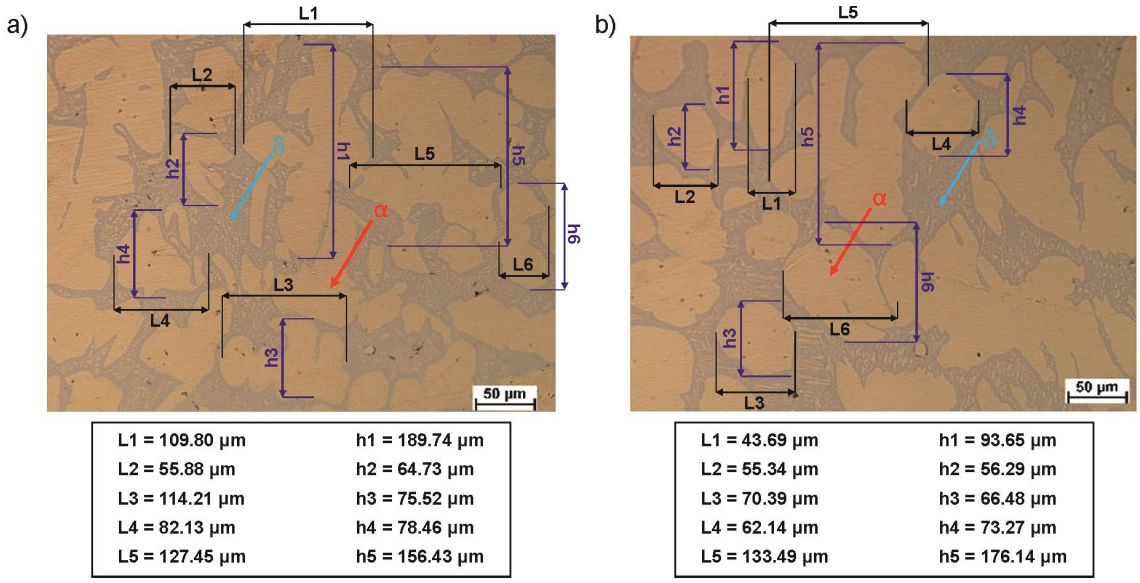

L1 = 109.80 µm	h1 = 189.74 µm
L2 = 55.88 µm	h2 = 64.73 µm
L3 = 114.21 µm	h3 = 75.52 µm
L4 = 82.13 µm	h4 = 78.46 µm
L5 = 127.45 µm	h5 = 156.43 µm

L1 = 43.69 µm	h1 = 93.65 µm
L2 = 55.34 µm	h2 = 56.29 µm
L3 = 70.39 µm	h3 = 66.48 µm
L4 = 62.14 µm	h4 = 73.27 µm
L5 = 133.49 µm	h5 = 176.14 µm

Fig. 9. Tin bronze microstructure a) furan resin form b) additive form with furan resin

compound. Both the change in the thermal conductivity of the mold and the change in the casting structure is most likely due to the difference in the amount of binder necessary to bind the sand grain. Additive technology forces the use of a much larger amount of binder than traditional casting methods.

REFERENCES

[1] O. Abdulhameed, A. Al-Ahmari, W. Ameen, S.H. Mian, Adv. Mech. Eng. **11** (2), (2019). DOI: https://doi.org/10.1177/1687814018822880

[2] C.W. Hull, Apparatus for production of three-dimensional objects by stereo-lithography. US Patent No. US5556590 A, (1996).

[3] C.R. Deckard, Method and apparatus for producing parts by selective sintering. European Patent No. EP0287657, (1989).

[4] T. Sivarupan, N. Balasubramani, P. Saxena, D. Nagarajan, M. El Mansori, K. Salonitis, M. Jolly, M.S. Dargush, Addit. Manuf. **40**, 101889 (2021). DOI: https://doi.org/10.1016/j.addma.2021.101889

[5] B. Lu, China Mech. Eng. **31** (1), 19-23 (2020). DOI: https://doi.org/10.3969/j.issn.1004-132X.2020.01.003

[6] S.R. Sama, J. Wang, G. Manogharan, J. Manuf. Proc. **34B**, 765-775 (2018). DOI: https://doi.org/10.1016/j.jmapro.2018.03.049

[7] D. Tachibana, K. Matsubara, R. Matsuda, T. Furukawa, S. Maruo, Y. Tanaka, O. Fuchiwaki, H.Ota, Adv. Mat. Tech. **5** (1), 1900794 (2019). DOI: https://doi.org/10.1002/admt.201900794

[8] M. Gao, L. Li, Q. Wang, Z. Ma, X. Li, Z. Liu, Int. J. Pr. Eng. Man-GT **9**, 305-322 (2022). DOI: https://doi.org/10.1007/s40684-021-00323-w

[9] J. Walker, E. Harris, C. Lynagh, A. Beck, R. Lonardo, B. Vuksanovich, J. Thiel, K. Rogers, B. Conner, E. MacDonald, Int. J. Metalcast. **12**, 785-796 (2018). DOI: https://doi.org/10.1007/s40962-018-0211-x

[10] P. Rodriguez-Gonzalez, P. Zapico, P.E. Robles-Valer, J. Barreiro, Addit. Manuf. **59A**, 103142 (2022). DOI: https://doi.org/10.1016/j.addma.2022.103142

[11] N. Hawaldar, J. Zhang, Int. J. Adv. Man. Tech. **97**, 1037-1045 (2018). DOI: https://doi.org/10.1007/s00170-018-2020-z

[12] S. Tang, L. Yang, Z. Fan, W. Jiang, X. Liu, China Foundry **18**, 249-264 (2021). DOI: https://doi.org/10.1007/s41230-021-1003-0

[13] L. Wang, X. Dong, S. Guo, China Foundry **18**, 344-350 (2021). DOI: https://doi.org/10.1007/s41230-021-1091-x

[14] K. Hu, H. Wang, K. Lu, Q. Feng, D. Yang, J. Cao, B. Zhang, Z. Lu, X. Ran, China Foundry **19**, 369-379 (2022). DOI: https://doi.org/10.1007/s41230-022-2048-4

[15] P. Kwiatoń, D. Cekus, M. Nadolski, K. Sokół, Z. Saternus, P. Pavlicek, Acta Phys. Pol. A **142** (1), 188-191 (2022). DOI: https://doi.org/10.12693/APhysPolA.142.188

[16] M. Nadolski, D. Cekus, The influence of casting parameters on the sound of a bell, in: METAL 2017: 26th International Conference on Metallurgy and Materials, TANGER LTD, 1893-1898, 2017.

[17] D. Cekus, P. Kwiatoń, M. Nadolski, K. Sokół, Eng. Sci. Tech. Int. J. **24** (4), 1042-1048 (2021). DOI: https://doi.org/10.1016/j.jestch.2021.01.012